Applied Energy 237 (2019) 862–872

Contents lists available at ScienceDirect

Applied Energy

journal homepage: www.elsevier.com/locate/apenergy

Life cycle assessment of hydrogen from proton exchange membrane water electrolysis in future energy systems

Kay Bareiß[a], Cristina de la Rua[a], Maximilian Möckl[b], Thomas Hamacher[a]

[a] Technical University of Munich, Department of Electrical and Computer Engineering, Chair of Renewable and Sustainable Energy Systems, Lichtenbergstrasse 4a, D-85748 Garching, Germany

[b] ZAE Bayern, Electrochemical Energy Storage, Walther-Meißner-Str. 6, D-85748 Garching, Germany

HIGHLIGHTS

- The paper provides a detailed inventory for a PEM water electrolyser system.
- An energy model was built to analyse the future energy mixes required by the system.
- LCIA results prove the relevance of the electricity mix for most impact categories.
- By 2050, the analysed system has less impact compared to the reference system.

ARTICLE INFO

Keywords:
Proton exchange membrane water electrolysis (PEMWE)
Life cycle assessment (LCA)
Energy modeling

ABSTRACT

This study discusses the potential of H_2 production by proton exchange membrane water electrolysis as an effective option to reduce greenhouse gas emissions in the hydrogen sector. To address this topic, a life cycle assessment is conducted to compare proton exchange membrane water electrolysis versus the reference process - steam methane reforming. As a relevant result we show that hydrogen production via proton exchange membrane water electrolysis is a promising technology to reduce CO_2 emissions of the hydrogen sector by up to 75%, if the electrolysis system runs exclusively on electricity generated from renewable energy sources. In a future (2050) base-load operation mode emissions are comparable to the reference system. The results for the global warming potential show a strong reduction of greenhouse gas emissions by 2050. The thoroughly and in-depth modeled components of the electrolyser have negligible influence on impact categories; thus, emissions are mainly determined by the electricity mix. With 2017 electricity mix of Germany, the global warming potential corresponds to 29.5 kg CO_2 eq. for each kg of produced hydrogen. Referring to the electricity mix we received from an energy model emissions can be reduced to 11.5 kg CO_2 eq. in base-load operation by the year 2050. Using only the 3000 h of excess power from renewables in a year will allow for the reduction of the global warming potential to 3.3 kg CO_2 eq. From this result we see that an environmentally friendly electricity mix is crucial for reducing the global warming impact of electrolytic hydrogen.

1. Introduction

Climate change is at the top of today's agenda in most countries and many policies have been put in place to face this global challenge. The European Union is approaching the deadline to reach the European 2020 climate and energy targets, but it has already established three new key targets for 2030: (i) reducing greenhouse gas (GHG) emissions at least by 40% compared to 1990 levels, (ii) increasing the share of renewable energy at least to 32%, and (iii) improving the energy efficiency at least to 27% [1]. Germany is a key player and aims to lead the European energy transition by setting even more ambitious objectives. The energy industry, in general, and the electricity sector, in particular, have been identified as targets due to their high contribution to GHG. In 2015, 37% of the energy-related GHG emissions were produced in the energy economy, followed by the transportation sector, which contributed with almost 18%. From the total amount of GHG emissions, 85% are related to the energy sector [2].

Electricity production in Germany from renewable energy sources accounted to 3% of the total share in 1990, while it represented already 32% in 2016 [3]. The country expects to cover 80% of its electricity demand from renewable energy sources until 2050 [3]. Most of this energy will be produced from solar and wind power. Besides the clear benefits of renewable energy sources for the environment, the integration of fluctuating energy sources in the energy system is still under discussion. Its availability depends on weather and season as well as on the time of the day. This intrinsic characteristic leads to situations in which electricity production exceeds electricity demand and the capacity of the electric system is surpassed [4]. Under these

https://doi.org/10.1016/j.apenergy.2019.01.001
Received 25 July 2018; Received in revised form 27 November 2018; Accepted 1 January 2019
Available online 15 January 2019

circumstances, energy storage is foreseen as one potential solution [5]. Schill [6] used an optimization model to determine the storage capacities required for taking up renewable surpluses under several scenarios in Germany with three storage options: batteries, pumped hydro storage and power-to-hydrogen. Taking into account the German expectations for 2050 in terms of renewable energy, the use of hydrogen can be seen as a promising solution [7,8]. Electrolytically produced hydrogen can help balancing the electric grid (storage), while also providing an energy carrier to be used in other sectors. A good example is the mobility sector. The need for decarbonizing mobility has placed hydrogen in a better position for future alternatives. Fuel cell vehicles (FCVs) convert hydrogen into electrical energy through a fuel cell. They do not emit any exhaust pollutant but water and have a longer driving range compared to battery electric vehicles (BEVs) [9–11].

Besides its potential for balancing the electric grid and decarbonizing the mobility sector, hydrogen is essential for a variety of industrial processes. Around 65 Mtons of hydrogen are produced yearly worldwide [12]. More than 90% of the hydrogen is used by two main industries, the petroleum recovery and refining industry (47%) and the ammonia production industry (45%) [13–15]. Hydrogen offers a versatility which makes it valuable for achieving the 2030 and 2050 targets from different perspectives. However, before deciding which pathways should be addressed first, it is necessary to study the whole supply chain of hydrogen production and to estimate the potential environmental impacts. This way it will be possible to identify critical issues and processes and propose measures to improve them. For that purpose, we present a life cycle assessment (LCA) of hydrogen production by proton exchange membrane water electrolysis (PEMWE) under different future energy scenarios.

2. Hydrogen production methods

Hydrogen can be supplied through several routes. A first division can be done based on the energy source used in the production. Hydrogen can be produced from both fossil energy sources and renewable energy sources [16]. To date, 48% of the hydrogen has been produced from natural gas, 30% from heavy oils and naphtha, and 18% from coal. From a technological perspective, there are four main production methods: (i) hydrocarbon reforming, (ii) hydrocarbon pyrolisis, (iii) biomass processing, and (iv) water splitting. Steam methane reforming (SMR) is the most common technology among the hydrocarbon reforming technologies, while electrolysis is the most established and well-known method in water splitting. The schematic processes of both SMR and electrolysis are shown in Fig. 1.

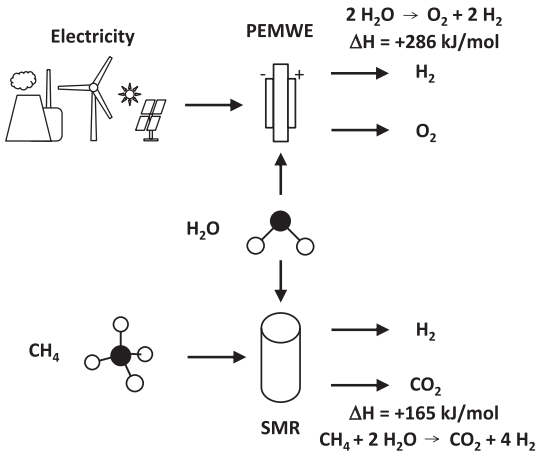

Fig. 1. Schematic drawing of the hydrogen production paths discussed in this paper. The focus is on PEMWE technology, SMR is used as a reference only. Electricity can be provided by renewables only or by a mixture of fossil power plants and renewables.

2.1. Steam methane reforming

The SMR method is a catalytic conversion of methane and steam to hydrogen and carbon dioxide. The method entails three steps: reforming or synthesis gas generation, water-gas shift and gas purification. The whole process happens under high temperatures and pressures up to 3.5 MPa. Eq. (1) shows the reforming process using methane as feed:

$$CH_4 + H_2O \rightarrow CO + 3H_2 \quad (\Delta H^0_{298} = +206\ \text{kJ/mol}) \tag{1}$$

In order to achieve a higher hydrogen yield a second step, the water-gas shift reaction, is used according to Eq. (2):

$$CO + H_2O \rightarrow CO_2 + H_2 \quad (\Delta H^0_{298} = -41\ \text{kJ/mol}) \tag{2}$$

The net reaction of the SMR process is the sum of Eq. (1) and (2):

$$CH_4 + 2H_2O \rightarrow CO_2 + 4H_2 \quad (\Delta H^0_{298} = +165\ \text{kJ/mol}) \tag{3}$$

With a net enthalpy of $\Delta H^0_{298} = +165$ kJ/mol the reaction is endothermic and needs external heat input. This is usually done by using natural gas (mainly methane) also as a fuel for heating. It is evident that in practice additional losses will occur. These are compensated by a higher methane consumption than theoretically necessary. The most significant loss is due to excess steam production [17]. The hydrogen production efficiency of a SMR plant can be defined as the power flux of the hydrogen produced divided by the power flux of the methane consumed:

$$\eta_{SMR} = \frac{p_{H_2}}{p_{fuel}} = \frac{\dot{m}_{H_2} \cdot LHV_{H_2}}{\dot{m}_{CH_4} \cdot LHV_{CH_4}} \tag{4}$$

The efficiency of exemplary industrial SMR plants calculated with Eq. (4) is around 74% [18,19]. Thus, the production of 1 kg H_2 leads to direct emission of about 8.8 kg CO_2. Taking into account not only the direct emissions from natural gas but the whole life cycle of the SMR, total CO_2 emissions are naturally higher.

2.2. Water electrolysis

Among the water splitting technologies, electrolysis is the most efficient method. The oldest and most mature type is the alkaline electrolyzer [20]. It consists of a cathode and an anode separated by a thin porous ceramic diaphragm submerged in an alkaline electrolyte. A newer generation of electrolyzers, also known as proton exchange membrane water electrolyzers (PEMWE), does not use a liquid electrolyte but a thin solid polymer electrolyte (membrane) instead [21]. This proton conducting membrane has a typical thickness of 60–200 µm. Nafion® is commonly used in commercial systems. On both sides of the membrane, thin electrodes of about 10 µm thickness are directly bonded to the surface. The electrodes contain noble metal catalysts, typically platinum-based at the cathode and iridium-based at the anode [22]. Some advantages of this technology are high energy efficiency, the provision of highly compressed and pure hydrogen and the flexible dynamic operation [23]. The still evolving PEMWE technology is currently more expensive compared to alkaline electrolyzers, mainly due to the use of critical and valuable materials such as titanium, platinum, iridium and the proton exchange membranes. Hence, there are current development efforts aiming to reduce their required amount [24]. The general operation process of a PEMWE cell is shown in Fig. 2. De-ionized water is supplied to the anode side of the cell. The membrane electrode assembly (MEA) is clamped between the porous transport layers (PTL) and the bipolar plates. The porous transport layers are typically carbon paper on the cathode side (thickness 280 µm, compressed) and sintered titanium foam or felt (thickness 280 µm) on the anode side [25]. The bipolar plates are made from titanium as well, and they usually feature channel-like structures (flow-field) for water and gas transport. In some designs, spatially stretched titanium mesh is

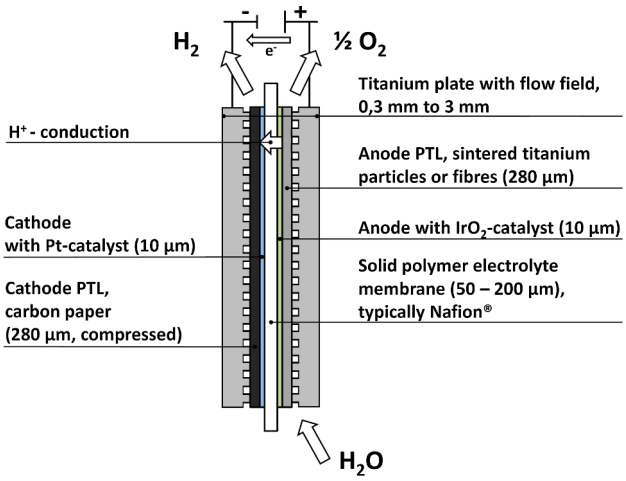

Fig. 2. Parts of a typical PEMWE cell.

also used to generate channels between the PTLs and the bipolar plates [26]. Titanium is one of the few materials which are suitable for the use on the anode side as it forms thin compact oxide layers, which are highly stable under the PEMWE operating conditions of low pH and high electrical potentials [27]. If a voltage greater than 1.23 V is applied to the cell, the necessary Gibbs free energy (ΔG^0_{298} = 237 kJ/mol) is supplied and the water is split with the integration of thermal energy from the environment. The value of (ΔG^0_{298} = 237 kJ/mol) is very close to the lower heating value (LHV = 242 kJ/mol) of hydrogen and thus is used synonymously in most publications [28]. For supplying the whole reaction enthalpy of (ΔH^0_{298} = 286 kJ/mol) a minimum voltage of 1.48 V is necessary. The cathode (negative terminal) produces hydrogen, while the anode (positive terminal) produces oxygen according to the following reactions:

$$\text{Anode: } H_2O \rightarrow \frac{1}{2}O_2 + 2e^- + 2H^+ \tag{5}$$

$$\text{Cathode: } 2H^+ + 2e^- \rightarrow H_2 \tag{6}$$

$$\text{Sum: } H_2O \rightarrow \frac{1}{2}O_2 + H_2 \quad (\Delta H^0_{298} = +286 \text{ kJ/mol}) \tag{7}$$

The protons are conducted from the anode to the cathode through the solid polymer electrolyte, whereas the electrons are driven through the external electric circuit. The cell's efficiency can be calculated from the cell voltage E_{cell} with the following equation:

$$\eta_{cell,LHV} = \frac{1.23V}{E_{cell}} \tag{8}$$

Under typical operating conditions, the cell voltages are between 1.5 V and 2 V [28]. The corresponding cell efficiencies are between 62% and 82% based on LHV. The PEMWE system efficiencies with all utilities (electronics, pumps, safety equipment, infrastructure, etc.) and faradaic losses included to deliver H_2 at industry grade 5.0 (99.999%) and 30 bar pressure are typically around 10–20% points lower than the cell efficiencies [29] and are in the range of 50–70% (LHV). As can be seen in Fig. 1, the direct CO_2 emissions of a PEMWE system are zero. However, from a life cycle analysis point of view, the use of this technology for hydrogen production is associated with certain CO_2 emissions. One important factor is the amount of emissions connected to the production of the input electricity.

2.3. LCA reference values for hydrogen production

As described above, many technologies are currently available for hydrogen production. They differ in many parameters, such as process efficiency and energy requirements. Taking into account this variety, it is understandable that a large amount of hydrogen's life cycle assessment was published during the last decade. Lee and colleagues [30] published recently the life cycle greenhouse gas emissions of hydrogen production as a by-product from chlor-alkali processes. Under different scenarios, hydrogen production creates 1.3–9.8 kg CO_2 eq. per kg of H_2. Utgikar and Thiesen [31] examined global warming and acidification impacts of a combined advanced nuclear-high temperature electrolysis plant. Producing 1 kg of H_2 leads to 2 kg of CO_2 equivalent (eq.) and 0.15 g H^+ eq. for each impact category. Cetinkaya [32] and her colleagues analyzed the global warming potential along the life cycle for five methods of hydrogen production. Electrolysis using wind emerged as the best option, emitting 0.97 kg CO_2 eq. per kg of H_2, followed by solar electrolysis, with 2.4 kg of CO_2 eq.. Conventional production of H_2 in a steam reforming process with natural gas would emit 11.9 kg of CO_2 eq. per kg of H_2. Dufour [33] also analyzed the impacts of electrolysis using different electricity technologies. From all analyzed sources, the production of H_2 using electricity from the grid leads to the largest GHG emissions, 28 kg of CO_2 eq. per kg of H_2 respectively. The study also assesses SMR with carbon capture and sequestration which results in 3.3 kg of CO_2 eq. In this direction, Verma and Kumar [34] estimated the GHG emissions of hydrogen production from underground coal gasification with and without carbon capture sequestration. Emissions were calculated to be 0.91 and 18 kg CO_2 eq. per kg of H_2.

Most articles focus on global warming potential, while few of them include other impact categories such as cumulative energy demand, acidification or eutrophication. One of them is the article published by Hajjaji [35], which compares eight alternative ways for hydrogen production including nine impact categories. Lastly, Wang and co-authors [36] have investigated GHG emissions along the life cycle of a new alternative to produce hydrogen, which couples chemical looping combustion with steam reforming. This technology would produce 3 kg of CO_2 eq. per kg of H_2.

In this regard, our paper aims to enlarge the current knowledge in the field from two different perspectives. Most reviewed articles provide aggregated data of the PEMWE stack. In this sense, we have made a big effort to describe each component of the stack as it is today and to estimate the future expected improvements based on the work developed in the Kopernikus project Power-to-X [37]. Besides, most studies analyze hydrogen production using a single energy technology as energy source, without considering the actual availability of that source within the energy system. In our study, we have integrated the life cycle analysis and an optimization energy model in line with the scope of the study. This way it is possible to understand how the energy system will react to the demand of hydrogen, and then to identify which energy sources will provide the energy required by the PEMWE.

3. Life cycle analysis

Life cycle assessment (LCA) is one of the most established methods for estimating the environmental performance associated to the life cycle of products and services. The first LCA framework was published by the Society of Environmental Toxicology and Chemistry [38]. After many modifications, the practice of LCA was regulated and nowadays its application follows the ISO 14040 and 14044 standards (ISOa, 2006 and ISOb, 2006).

The LCA comprises four phases: (i) goal and scope definition, (ii) inventory of inputs and outputs, (iii) impact assessment, and (iv) interpretation of results. This study will address the four stages as established in the ISO standards.

3.1. Goal and scope of the study

The main objective of this study is to quantify the potential environmental impacts of hydrogen produced by PEMWE in Germany under different energy scenarios. The LCA has been modeled from an

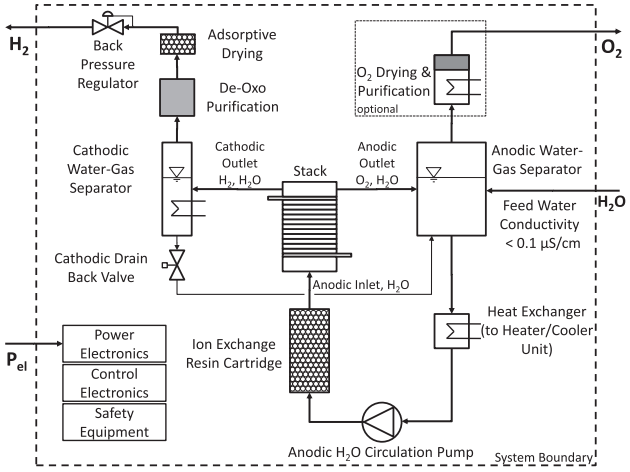

Fig. 3. Scheme of the analyzed PEMWE system layout showing all essential parts for hydrogen 5.0 production at 30 bar pressure, modified from [39,40]. The anode gas drying and purification system is optional and not necessary unless the produced O_2 is used as well.

attributional approach as a cradle to gate system. However, it must be noted that systems outside these boundaries might be affected by the new demand of hydrogen. This is the case of the German electric system. In order to reflect these consequences, the study includes results from an energy model, described in Section 4, which will reflect the potential German electric system under the new demand of H_2. Fig. 3 shows the processes and components included within the system boundaries. The chosen functional unit is defined as 1 kg of dried hydrogen produced in Germany in a PEMWE plant, with a standard quality of 5.0 and 30 bar pressure at 60 °C operating temperature. First, de-ionized water is fed to the anode water-gas separation tank. To avoid certain system degradation issues, water conductivity has to be lower than 0.1 µS/cm [41]. The water is pumped to the cell stack, the core part of the system. Previous to the stack there is an ion exchange resin cartridge for maintaining a low water conductivity. The water leaves the stack at the anode outlet together with the produced oxygen. It is cycled back to the water-gas separation tank. A heat exchanger in the anodic cycle allows the system to maintain a certain working temperature. Typically the working temperatures are in a range between 60 °C and 80 °C [42]. The produced oxygen is usually vented. Gas treatment of the oxygen (drying and purification) is only done if the oxygen is used in a subsequent process. The water circulation is done on the anode side. On the cathodic side of the stack in most cases no water cycling is necessary because there is a net transport of water from the anode to the cathode during operation due to the electro-osmotic drag [43]. Hydrogen and water leave the stack at the cathodic outlet. The gas-water mixture is cooled down close to ambient temperature and liquid water is separated and drained back to the anodic water-gas separation tank. The water-saturated hydrogen is fed to a catalytic de-oxo purification device to reduce the oxygen content to a level of less than 5 ppm. A subsequent adsorptive dryer finally reduces the water content to values lower than 5 ppm [29]. The pressure on the cathodic side typically can reach up to 30 bar. In most cases, the oxygen side is kept at ambient pressure for easier system design and less cross permeation [44]. Further obligatory system components are the power electronics (rectifier and voltage transformer), control electronics and safety equipment. In many applications the whole PEMWE system is integrated in standardized 20 ft or 40 ft containers as depicted in Fig. 4. The balance of plant (BOP) lifetime is assumed to be 20 years [45].

Although the technology is already quite developed, it is expected to further improve in the near future. In addition, the energy mix in Germany will also vary its current configuration to fulfill the policy targets. For this reason, we have extended the initial time horizon from

Fig. 4. Typical containerized PEMWE system in the 1 MW power range at Windgas Hamburg, Reitbrook project site. (Copyright ©Uniper SE).

2017 to 2050, so that our results can reflect these changes.

Data for the foreground system has been collected from different sources. An important part of the data has been taken from laboratory measurements and was reviewed by several industrial partners. Other sources, such as literature review, scientific articles and technical information from commercial sources, have been used when necessary.

Data for the background system has been taken from the ecoinvent v3.3 database. Whenever the available datasets provided in the database did not reflect the geographical and time horizon previously defined in this study, they were modified using additional information. The analysis has been modeled using the software SimaPro. There are currently a large variety of impact assessment methods. The Joint Research Centre (JRC) published in 2011 an extensive review of different methods using criteria such as completeness of the scope, environmental relevance and scientific robustness among others [46]. As result of this review, they proposed an umbrella method, which comprises the best scored method for each impact category. Although the use of this method could be appropriate, we have chosen the most updated version of the ReCiPe Midpoint method to carry out this study [47]. Some of the weaknesses highlighted by the review from the JRC report have been surpassed in the most updated version. Besides, by using one unique method for all impact categories, we can assume that the underlying limitations and assumptions for each category are consistent with each other. The following impact categories have been included in the analysis:

- Climate change (CC)
- Ozone depletion (OD)
- Terrestrial acidification (TA)
- Human toxicity (HT)
- Particulate oxidant formation (POF)
- Particulate matter formation (PM)
- Metal depletion (MD)

3.2. Life cycle inventory

This section describes the different processes within the system boundaries. Inventory data are shown as well in this section, together with the main assumptions and hypothesis taken along the study.

3.2.1. PEMWE stack

The stack as the core component of a PEMWE system is basically a connection of several single cells in series. This is schematically shown in Fig. 5.

The individual cells of the same principle as shown in Fig. 2 are separated by titanium bipolar plates. At the upper and lower end of the

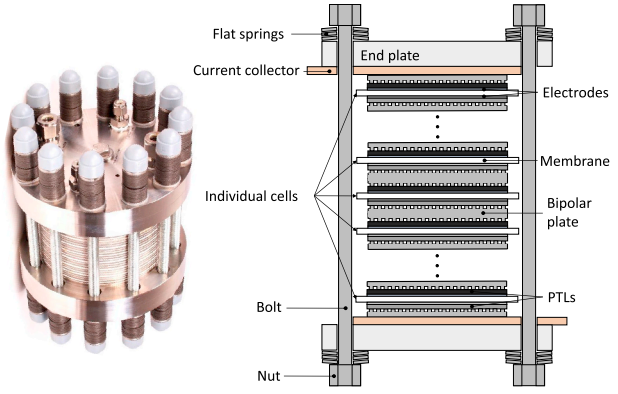

Fig. 5. Picture and simplified schematic drawing of a PEMWE stack of the lower power class up to 100 kW. More powerful systems in the MW class are very similar in their components, the main difference is the size of the active cell area. (Picture: Copyright ©HIAT gGmbH).

cell stack current collectors, mainly made of copper or aluminum [25], are installed for the electrical connection. Thick end plates made of aluminum or steel together with several bolts and sets of stacked flat springs are used to ensure an even compression of the cells. The stack lifetime of commercial systems is typically 40000–60000 h and is planned to reach 90000 h or roughly 10 years of continuous service in near future systems [24]. The main parts prone to degradation are the MEA and the anodic PTL [48]. These can be substituted by new components in an overhaul process.

Table 1 shows an overview over some key parameters of the PEMWE system, which are important for the LCA. Current state-of-the-art values (2017) and their estimated development for the near future are gathered. Today's mean cell efficiencies are 70% at corresponding cell voltages of 1.79 V and current densities of around 1.5 A/cm^2 [28]. The system efficiencies including all utilities are about 10 percentage points lower at 60% [28]. Typical anode catalyst loadings are 2 mg/cm^2 iridium [22]. In contrast, the cathode catalyst loadings are about ten fold lower with 0.2 mg/cm^2 platinum. This is possible as the cathodic reaction kinetics are several orders of magnitude faster [49]. The titanium bipolar plate thickness in current state-of-the-art PEM electrolyzers is about 3 mm [50] as there are machined or etched channels on both sides of the bipolar plates with depths of about 1 mm each [51]. Polysulfonic acid membranes for proton conduction (mostly Nafion®) with thicknesses of about 200 µm are used as electrolyte [42].

Research efforts are undertaken to intensify the current density and to lower the catalyst loadings while keeping the high efficiency level [42]. Also, design improvements are expected to reduce the material usage, especially of the expensive and difficult to manufacture titanium bipolar plates. Possible ways to achieve these goals are presented in the following:

Table 1
Current and estimated near future PEMWE system parameters.

Parameter	2017	Near future
Cell voltage level (V)	1.79	1.79
Current density (A/cm^2)	1.5	3
Power density (W/cm^2)	2.7	5.4
η_{cell} (LHV)	0.7	0.7
η_{system} (LHV)	0.6	0.6
Anode Ir. loading (mg/cm^2)	2	0.2
Cathode Pt. loading (mg/cm^2)	0.2	0.05
Ti. bipolar plate thickness (mm)	3	0.3
Membrane thickness (µm)	200	50
Single cell format (cm^2)	500	1000
Stack lifetime (years)	7	10
BOP lifetime (years)	20	20

- Reduced catalyst loadings: At the cathode for the hydrogen evolution reaction (HER), the platinum loadings can be reduced by a factor of 8 from today 0.2 mg_{Pt}/cm^2 to 0.025 mg_{Pt}/cm^2 without significantly influencing cell performance [52]. With a security factor included for possible degradation issues, 0.05 mg_{Pt}/cm^2 seems a reasonable value for cathode loadings for the near future. At the anode, the oxygen evolution reaction (OER) is much slower and therefore more catalyst surface area is necessary. As iridium is only mined in a quantity of approximately 4 t/y [42], it was estimated by Bernt et. al. that the power specific iridium loading should get down to 0.01 g_{Ir}/kW at efficiencies similar to today's (≈ 70%) so PEMWE can be used on a large scale with about 150 GW installation per year [52]. By using improved catalysts with higher surface area, a ten fold reduction of the iridium content down to 0.2 mg_{Ir}/cm^2 at increased current densities of 3 A/cm^2 is assumed to be possible in the near future.
- Thinner membranes: A reduction of membrane thickness from 200 µm to 50 µm in the coming years seems a possible goal. Experimental tests with thinner membranes showed good results [25]. Similar reductions of membrane thickness were achieved in PEM fuel cell technology [53,54]. This facilitates an operation at higher current densities, as the ohmic resistance of the cell is significantly reduced [42]. At the same time, it has to be ensured that the permeation losses and degradation processes are not increasing too much with the thinner membranes [55,56].
- Thinner bipolar plates: Bipolar plates can be produced faster and with less material usage by forging of thin sheet metal instead of destructive milling or etching of thicker base material. Similar approaches were done in PEM fuel cell technology, where sheet metals with thicknesses of 50 µm are stamped or forged to manufacture flow fields [57]. In PEMWE systems, with higher operating pressures and thus tighter mechanical restrictions of the minimum bipolar plate thickness, possible reductions are assumed to be ten-fold down from initial 3 mm [50] to 0.3 mm in the near future.

3.2.2. Gas purification

After passing the cathodic water-gas separator unit the produced hydrogen is saturated with water vapor. The water vapor pressure depends on the water-gas separator temperature. In most cases, this device is cooled down slightly above ambient temperature. Average values are assumed to be about 20 °C which corresponds to a water vapor pressure of 23 mbar. At the cathode, total pressures of 30 bar result in a water vapor content of about 770 ppm or 7 g H_2O per kg of H_2. Some oxygen is also present in the cathodic product gas due to permeation processes across the membrane. According to findings by Trinke et al. [58] the mean oxygen impurity level is estimated to be about 800 ppm. For removing these impurities, a de-oxo unit is used, which catalytically cold burns the oxygen traces with hydrogen to water. The produced water from the de-oxo unit, together with the water vapor from the water-gas separator, is reduced to less than 5 ppm by a subsequent adsorptive drying process.

- De-Oxo
  Different types of de-oxo purification units are available on the market. One possibility is the use of platinum group metals to remove the oxygen content in the hydrogen gas stream in a catalytical recombination device. The reaction is as follows:

$$2H_2 + O_2 \rightarrow 2H_2O \quad (9)$$

  While removing the 800 ppm of oxygen, about 15 g of H_2O is produced per kg of H_2. The product water from the de-oxo device together with the 7 g of H_2O per kg of H_2 from the gas-water separator is subsequently removed in an adsorption process.
- Adsorption Process
  In most applications, silica gel is used as adsorbent. The silica gel adsorbs water at its surface until it is completely covered and

Table 2
Materials for a 1 MW PEMWE stack, state-of-the-art and near future.

Material (kg)	2017	Near future
Titanium	528	37
Aluminum	27	54
Stainless steel	100	40
Copper	4.5	9
Nafion®	16	2
Activated carbon	9	4.5
Iridium	0.75	0.037
Platinum	0.075	0.010

saturated [59]. Silica gel needs to be baked out before it can be used again. Thus, to maintain a continuous drying process, two silica tanks in a batch process are considered in the study. Energy and material requirements to produce silica gel have been taken from the literature [60]. Between 7100 and 8400 kJ are required to evaporate 1 kg H_2O from silica [59]. This results in an energy demand of 0.05 kWh per kg dried H_2 at 30 bar pressure.

The life cycle inventory (LCI) has been collected for each described process. Taking into account the system parameters for 2017 and the near future shown in Table 1, the required materials for a 1 MW stack have been estimated. The total active cell area for a 1 MW stack is 37 m^2 for state of-the-art and 18.5 m^2 in the future. Subsequently, the material quantities have been estimated assuming a simple layered design as shown in Figs. 2 and 5. Quadratic cell formats with active areas of 500 cm^2 for 2017 and 1000 cm^2 for the near future are chosen for estimating the size of the endplates and current collectors. Based on demonstration systems, the end plate thickness is assumed to be 10 cm and the current collector thickness to be 5 mm. Furthermore, the mass of the stainless steel bolts and screws is conservatively estimated. The mass of sealing material and inlet and outlet fittings has been neglected. Table 2 contains the LCI of the main materials for the state-of-the-art and future 1 MW stack.

Titanium is the material that contributes the most to the total mass of the stack in its current configuration. The need for a reduction of its use is mainly driven by its high cost [61] and the difficulty of machining or etching thick titanium bipolar plates. It can be noticed that the effect of higher power density, reduction of the bipolar plate and membrane thickness and reduction of catalyst platinum group metal loadings will lead to a strong decrease in material usage. Especially the application of cost intensive materials like iridium, platinum and also titanium and Nafion® is reduced by 85–95%. Only for the construction materials aluminum and copper a higher usage can be assumed for the future as the active cell area format is doubled.

3.2.3. Balance of plant

The BOP materials are more difficult to estimate, as there is only few publicly accessible information from PEMWE system manufacturers, in most cases only in form of technical specifications as in [62–64]. However, a rough estimation for the materials with a high safety margin is attempted in the following. The assumed system is a containerized solution in a standard 20 ft container with a structural weight of 3.9 t. The foundation is made from concrete realized by 4 point-foundations with a thickness of 25 cm each and a squared area of 1.5 m edge length. The total weight of concrete for the foundation amounts to 5.4 t. To ensure a sufficient water flow, a pump with 10 kW is required. The power electronics, which includes the rectifier and the voltage adaption, weighs 1 t and the control electronics accounted for 100 kg of gross mass. In addition, some construction and process material such as steel elements, plastic and stainless steel piping, adsorbents and lubricants are included in the analysis. The integrated system materials and their estimated masses are specified in Table 3. Fig. 6 shows the mass shares of the BOP components and the PEMWE stack for 2017. It is clearly visible that the highest mass share (78%) refers to construction elements (foundation, steel construction, container) whereas only 5% is used for the actual electrochemical device, the PEMWE stack.

Table 3
Main materials and assumed masses of the PEMWE BOP.

Materials	Mass (t)
Low alloyed steel	4.8
High alloyed steel	1.9
Aluminum	< 0.1
Copper	< 0.1
Plastic	0.3
Electronic material (power, control)	1.1
Process material (adsorbent, lubricant)	0.2
Concrete	5.6

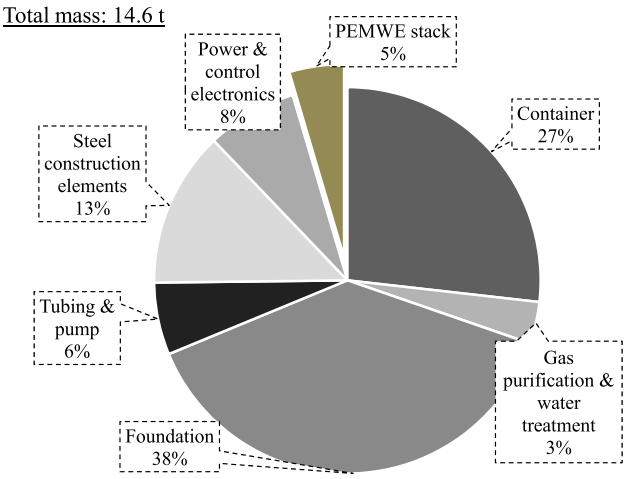

Fig. 6. Mass shares of the components belonging to the electrolyzer system (2017).

4. Energy scenarios

After the static PEMWE system has been described, we investigate the dynamic plant operation. Water splitting is an energy demanding process using electricity and some heat. In our system, the heat is also provided by electricity. From stoichiometry results, we know that 9 kg H_2O are required for producing 1 kg H_2. In addition, 55 kWh of electricity are necessary for water splitting at an efficiency of 60% LHV. The choice of energy sources has an important impact on the results as shown by Valente et al. in their extended reviews [65,66]. The energy sources determine the GHG emissions as well as the cumulative energy demand (CED) of the whole life cycle. The potential effects of the electricity mix on our final results make a more detailed analysis of the current and expected development of Germany's energy system necessary. There are numerous studies focusing on energy modeling in Germany [67–70]. However all of them have their own assumptions on different aspects which are not in line with our scope of research. In addition most available studies are published in an aggregated and already interpreted form, which do not provide the necessary degree of freedom. In our premise, we see FCVs as an important component in the course of the energy transition concerning the mobility sector. For this reason, an amount of H2 requirement was assumed, which is covered by the PEMWE. The capacity expansion of PEMWE and the use of available storage capacities, however are determined endogenously, taking into account the hourly optimized electricity mix by the model. In order to illustrate this complex approach, a linear optimization problem tailored to this research question has been set up. We have built an energy model to computationally answer the question about a

future power mix. A linear optimization problem was described with the open source model-generator "urbs" [71], which was created at the chair of "Renewable and Sustainable Energy Systems" at TUM. The model consists of 16 nodes (for every state of Germany) and does not allow international energy exchanges. Each region (node) is connected to its surroundings with transmission lines. Energy demands (electricity and hydrogen) are given, which have to be covered by different technologies. Three premises were set:

1. A largely electrified private traffic is assumed to match the goal of decarbonization in the private transportation sector. The analysis of the average distance kilometers traveled per trip is based on reference to [72]. Journey distances shorter than 250 km have been assumed to be suitable to be operated by BEV. Due to the limited battery capacity and longer charging time of BEV, hydrogen vehicles are more suitable for longer journeys [73]. Thus, remaining mileage is satisfied by FCV. The electricity requirement of BEVs is added proportionally to the general electricity demand. The battery storage of the vehicles is not included in the power grid as storage. From the analysis, we state 71% of the mileage is provided by BEVs accordingly remaining mileage demand is covered by FCVs. BEVs have an overall higher rate of efficiency (0.57 MJ/km) compared to FCVs (0.73 MJ/km) [67]. Electricity consumption for BEV accounts to 60 TWh, while covering H_2 demand including the efficiency of the PEM system amounts to 35 TWh.
2. The tolerated CO_2 emission limits is made up of the sectors energy economy and private traffic in 2050. Total CO_2 emissions are 80% lower compared to 1990 emissions from private transport (19 Gtons) and energy economy (43 Gtons).
3. The maximum installable capacity of wind is calculated by the share of non-occupied land like settlements, rivers or roads, in Germany. From this share we assume an occupancy of 5% of suitable space in Germany as not all useful space will be allocated to wind farms. By assuming 5 MW turbines in 250 m distance each, a potential of 20 MW/m^2 is available, which corresponds to 198 GW onshore capacity. This value is slightly higher than the 178 GW stated in [74] (Scenario: "Energiewende- Referenz") but much lower than the 930 GW from [75] as they allow a higher share of Germany for wind-farming. The quality of a wind location is characterized by the amount of full load hours of their corresponding wind time series [76]. 1/3 of the capacity is assigned to very good wind locations (the best third of each region). As a simplification, the remaining 2/3 are assigned to the second best third of wind locations. The maximum capacity of photovoltaic systems is not limited. The use of conventional power plants is determined by the model.

To cover the energy demand, 0.1 TWh pump storage and 0.5 TWh hydrogen storage are set as readily installed. The hydrogen storage represents the capability of existing fuel storage as our hydrogen demand results from FCVs. The efficiency of FCV is given with 0.73 MJ/km [78] and for BEV (300 km range) 0.57 MJ/km [67]. The model solves the problem cost optimally on an hourly time base by keeping the direct maximum CO_2 emissions under a given limit. Finally, we investigated the specific CO_2 emissions of the hourly electricity mix which is plotted in Fig. 7. From the curve, we stated two different operation modes of PEMWE and therefore two load profiles. For a future hydrogen production via PEMWE, based solely on renewable energy, we get 3000 full load hours as a result. The operation time will increase to 8760 h when 40% of the energy is supplied by combined cycle gas turbine (CCGT). All assumptions and further details are published in a working paper [77]. The results from the two different scenarios are shown in Table 4.

5. Results and discussion

In this section we present the potential environmental impacts

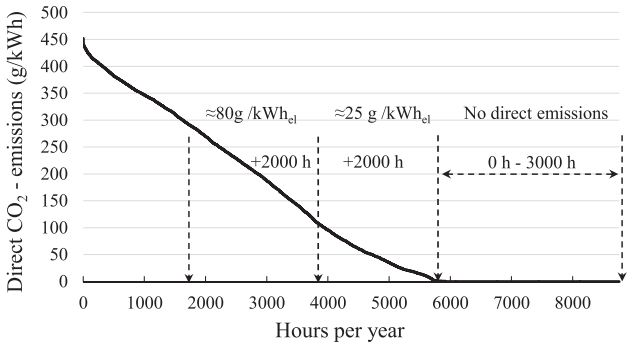

Fig. 7. In descending order sorted CO_2 emissions curve; only direct CO_2 emissions from burning fossil fuels in conventional power-plants are taken into account. Energy from renewables do not have any emissions in the model (figure taken from [77] and translated).

Table 4
Share of power generation from the different scenarios (%).

Power plant	2017 baseload [79]	2050 baseload [77]	2050 3000 h [77]
Hard coal	15	0	0
Lignite	24	0	0
Nuclear	12	0	0
Natural gas	14	40	0
Oil	1	0	0
Wind enery	17	39	65
Photovoltaic	6	21	35
Biomass	8	0	0
Hydro power	3	0	0

associated with the production of hydrogen by a PEMWE under three different energy scenarios from a life cycle approach. The electricity mixes resulting from the energy model for the different scenarios are shown in Table 4. For today's electricity mix, the GWP is 29.5 kg CO_2 eq. for each kg of produced hydrogen as shown in Fig. 8. This amount is reduced by 60% if the electricity required by the system is produced as described in the 2050 base-load operation scenario. In this case, the production of 1 kg hydrogen causes the emission of 11.5 kg CO_2 equivalent. The most favorable scenario (3.3 kg CO_2 eq.) assumes that

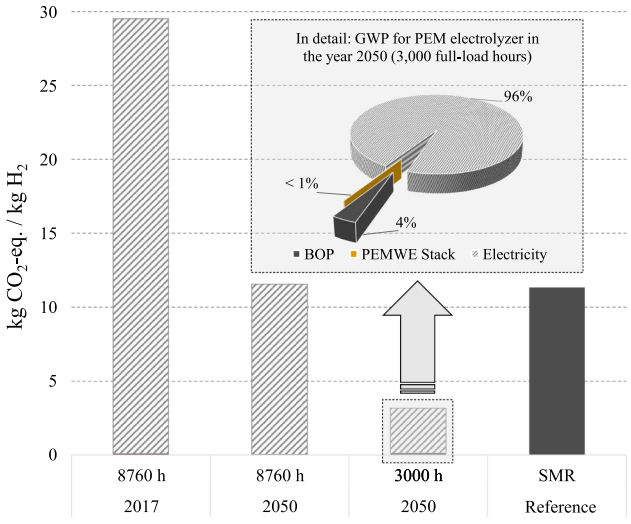

Fig. 8. Global warming impact from CO_2 emissions of the PEMWE system. Emissions are separated into BOP, PEMWE Stack and Electricity. As BOP and PEMWE Stack contribute with a maximum of 4% to the GWP, a pie chart is added in the case of the scenario with 3000 full-load hours.

the PEMWE is operating 3000 h using only electricity produced by renewable sources. Fig. 8 also shows the contribution of the different system components to the GWP for the best case. The modeled components of the PEMWE stack (near future design) have negligible influence, with less than 1%. The PEMWE BOP accounts for only around 4% while the electricity supply is responsible for 96% of total GHG emissions. The contribution of the PEMWE stack and BOP is even lower for the other scenarios. Comparing our results with Bukhardt et al. [80], a distinctly higher proportion of nearly 20% is attributable to the electrolyzer's manufacture supply chain. This divergence can be explained, beside the material choice, by the lower power density of alkaline electrolyzers [28], the system is correspondingly larger than a PEMWE. A comparison of the mass balance shows that the alkaline electrolyzer (including foundation) weighs, with 30 tons, twice as much compared to the PEMWE system examined in this study. Thus, hydrogen production by PEMWE with its high power density should result in lower GWP compared to alkaline electrolysis when using the same input electricity. Although the production of hydrogen in a SMR process is out of the scope of our study, in the figure we have included the GHG emissions associated to this technology (11.5 kg CO_2 eq./kg of H_2) in order to have a reference value. This value has been extracted from the GaBi database.

Since hydrogen as fuel is a premise of our energy scenario, we briefly describe how FCV can contribute to a sustainable transportation sector for the year 2050. First of all, FCVs are more efficient (0.73 MJ/km compared to internal combustion engine (1.2 MJ/km) [67]. Secondly, GWP of gasoline is around 84 g CO_2 eq. per MJ [81], which results in 101 g CO_2 eq. per vehicle kilometer (vkm). Hydrogen from PEM, even in base-load operation (11.5 kg CO_2 eq./kg of H_2) leads to 70 g CO_2 eq. per vkm (hydrogen from SMR will result in similar results). Using the flexibility of PEMWE and matching the hydrogen production with the fluctuating power generation of renewables (3000 h) will further reduce the emissions to 20 g CO_2 eq per vkm.

The change of energy sources in the electricity mix over time does not only contribute to the reduction of GWP but also to the cumulative energy demand indicator. This indicator serves as reference to measure the system's efficiency in terms of energy consumed and produced, considering the whole supply chain. The aim is not only to decrease the CED of the system, but also to decrease the contribution of non-renewable energy sources. Therefore, in this paper we distinguish between renewable and non-renewable cumulative energy demand. The result for the cumulative energy demand of the individual operating modes is shown in Fig. 11. In the base scenario (2017), the production of 1 kg hydrogen requires around 550 MJ along the whole system. Under the second and third energy scenarios, the CED is reduced by 23% and more than 53%, respectively. Producing 1 MJ of H_2 requires around 4.6 MJ along the supply chain in the current scenario, but only 2.1 MJ in the best case scenario, 2050 (3000 full load hours). When analyzing the indicator divided into the two subcategories, renewable and non-renewable, it is possible to perceive that besides an improvement in energy efficiency, there is also an increase in renewable energy source's contribution to the cumulative energy demand. In the current situation, 77% of the CED has a non renewable source, which includes fossil and nuclear energy. This value decreases by 15% when the electricity is produced under the 2050 scenario with 3000 full load hours. As in the case of GWP, we have included the CED from SMR as reference. Although this process demands lower cumulative energy along the supply chain compared to any other scenario, 99% of this energy has a non renewable origin. Table 5 shows the potential environmental impact for each impact category under the three energy scenarios. It can be noticed that the highest values for most categories occur in the current scenario. However, there are two categories in which the trend is different. Human toxicity decreases due to the phase-out of lignite in scenario 2050 (8760 h) compared to the current scenario, but it increases again in 2050 (3000 h) because of the high demand of copper for the wind turbines. In the case of metal depletion,

Table 5
Impact categories for PEMWE in 2017 and 2050.

Impact (unit)	2017 baseload	2050 baseload	2050 3000 h
CC (kg CO_2 eq.)	29.5	11.6	3.0
OD (10^{-6} kg CFC-11 eq.)	2.6	2.6	2.3
TA (10^{-2} kg SO_2 eq.)	4.7	2.5	2.1
HT (kg 1,4-DB eq.)	24.8	3.9	5.6
POF (10^{-2} kg NMVOC)	3.4	2.0	1.3
PM (10^{-2} kg PM10 eq.)	1.6	1.2	1.1
MD (kg Fe eq)	0.53	0.93	1.5

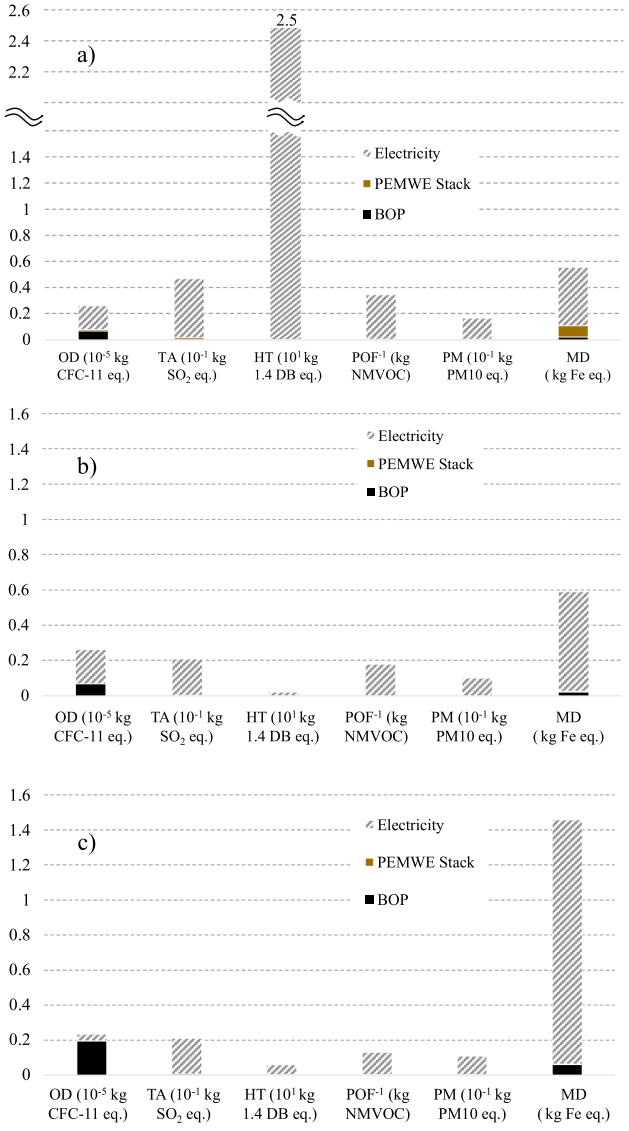

Fig. 9. Impact assessment results per functional unit from the following scenarios: (a) 2017, (b) 2050 (8760 h), (c) 2050 (3000 h).

the potential impact is larger both in 2050 (8760 h) and 2050 (3000 h). Although there is an important reduction of metals (titanium, iridium) used in the PEMWE stack from 2017 to 2050, total MD increases due to the higher share of wind (copper) and PV (silicon, iron) energy in the electricity mix. From these results shown in Fig. 9, we see that the electricity mix is crucial for reducing most environmental impacts, although it might lead to the increase of some other categories. In order to better understand the reasons behind these effects, it is necessary to further investigate the impacts of each energy technology in each

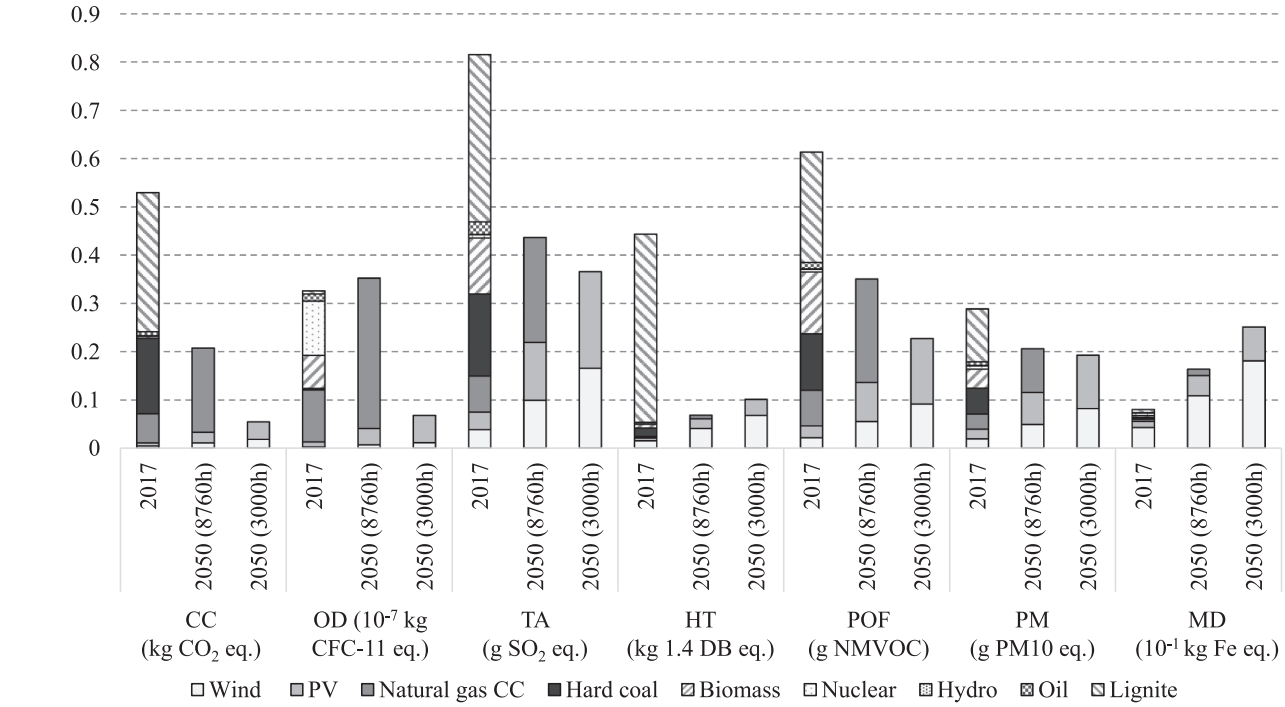

Fig. 10. Further environmental impacts. All impact categories are related to 1 kWh electricity.

energy scenario.

Fig. 10 shows the potential environmental impacts of producing 1 kWh of electricity in each energy scenario, taking into account the different contribution of each energy technology. As expected from the results shown in Table 5, most environmental impacts associated with the production of 1 kWh of electricity decrease in the energy scenarios with higher share of renewable energy sources. In 2017, the environmental impacts are mostly associated with fossil energy sources such as lignite and hard coal. Biomass and natural gas also contribute to the acidification potential and photochemical ozone formation. In the energy scenario 2050 (8760 h), all impacts are driven by natural gas. In some categories, such as climate change or ozone depletion, this energy technology represents more than 90% of the total impact, while in other categories, such as acidification potential or particulate matter, its contribution does not exceed 50%. Lastly, in 2050 (3000 h), the lack of natural gas as energy source leads to the reduction of most environmental impacts. With a share of 35%, solar energy plays an important role in most categories except in metal depletion, mainly associated with wind energy.

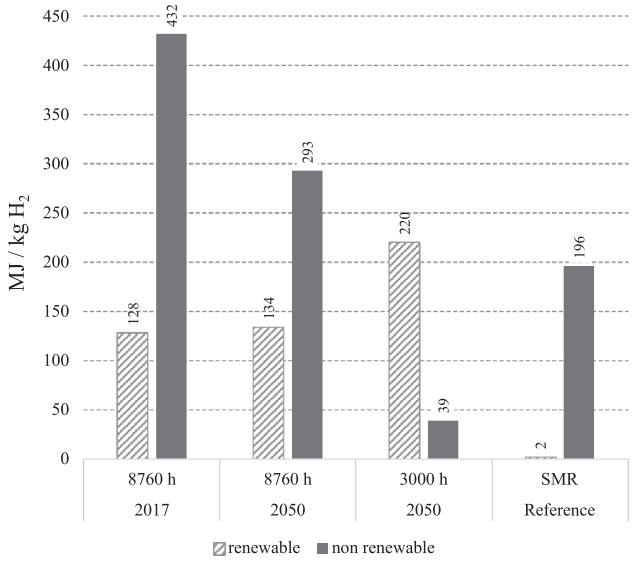

Fig. 11. A significant reduction in energy from non-renewable is observed starting from 2017 until 2050. In contrast to that, the amount of energy from renewable sources is only rising moderately.

Besides the potential environmental impacts included in a classic LCA, the use of critical materials in the supply chains has recently become a new important topic. The European Commission periodically renews the list of critical materials. These depend on several parameters. The most important are:

- The importance of the material to the EU economy in terms of the cost of material substitution (SIEI Index).
- The security of supply by the supplying regions depending on the development of the respective government and trade performance.

Favorable substitution possibilities or reprocessing of these critical raw materials have a risk-reducing effect on their evaluation in the considered life cycle [82]. The platinum group metals are identified as critical raw materials [83] in this study. It is estimated that the use of iridium in the PEMWE stack can be reduced by 90% by 2050. The platinum loading is reduced by 75%. To cover the H_2 demand from the energy model an installed PEMWE power between 7 GW in full-load and 20 GW in the 3000 h scenario is necessary. With a typical stack lifetime of 7 years the iridium demand (excluding recycling) is between 0.8 t and 2.1 t per year in Germany only. In contrast, the average worldwide production rate of iridium, which is a co-product of platinum, is between 3.5 t [84] and 4 t per year [42]. Therefore, it is crucial to reduce their amount if PEMWE is seen as a roll-out technology for future energy systems. In addition FCV will need a certain amount of platinum for their fuel cell stacks. However, this is outside our system boundaries.

6. Conclusion

We have reported that for different impact categories of hydrogen produced by proton exchange membrane water electrolysis, the

influence of system components plays a minor role. Our investigation has shown that mainly the composition of the electricity mix determines the impacts like global warming potential. A reduction of the used materials causes only very little reduction in global warming potential. Nevertheless, there is a clear influence of material reduction on the critical materials. Three different operation modes of the proton exchange membrane water electrolysis were investigated; for each, a specific process electricity was developed. Further investigation shows that hydrogen production with proton exchange membrane water electrolysis in the future (2050) is definitely an alternative to conventional steam methane reforming production. However, the operation mode by proton exchange membrane water electrolysis is flexible enough for fitting into hours with volatile electricity production having very high shares of renewables. Due to the flexibility of the plants, proton exchange membrane water electrolysis can play an important role in integrating renewables. With the appropriate storage capacity, surplus of hydrogen produced can be used for later re-conversion to stabilize future energy systems or as fuel for fuel cell vehicle. By subsidizing fossil oil in the private transportation sector, even in the baseload scenario, global warming potential is reduced by 30%. Due to the capability of flexible load behavior, proton exchange membrane water electrolysis can contribute to a high reduction of greenhouse gas emitted by the transportation sector by up to 80%, as we have shown. However, our results are subject to the restriction of using existing databases for the background data. These data are based on state of the art or based on older processes. In order to depict future value chains, which also use electricity in production steps, these data sets would also have to be updated for reasons of consistency which is outside of our focus. Therefore, feedback effects of future energy mixes regarding indirect emissions cannot be taken into account. For further investigations of innovative technologies, new datasets should be created which allow increases of efficiency in the production of energy production technologies e.g. solar panels through a lower emission factor of used electricity. This would further reduce the global warming potential of renewable hydrogen production by proton exchange membrane water electrolysis.

Acknowledgement

The authors gratefully acknowledge funding by the German Federal Ministry of Education and Research (BMBF) within the Kopernikus Project P2X: Flexible use of renewable resources – exploration, validation and implementation of ‘Power-to-X’ concepts.

References

[1] Rat E. Tagung des Europäischen Rates (23./24. Oktober 2014) – Schlussfolgerungen, Tech. rep., Europäischer Rat, 2014. URL:<https://www.bundesregierung.de/Content/DE/Reiseberichte/2014-10-22-europaeischer-rat-oktober.html>, [accessed June 27, 2018].
[2] Strogies M, Gniffke P. Berichterstattung unter der Klimarahmenkonvention der Vereinten Nationen und dem Kyoto-Protokoll 2017. Tech. rep., Umweltbundesamt; 2017.
[3] BMUB M, Weiß MW. PtJ, Klimaschutz in Zahlen Fakten, Trends und Impulse deutscher Klimapolitik, Tech. rep., Bundesministerium für Umwelt, Naturschutz, Bau und Reaktorsicherheit (BMUB); 2017.
[4] Hart EK, Stoutenburg ED, Jacobson MZ. The potential of intermittent renewables to meet electric power demand: current methods and emerging analytical techniques. Proc IEEE 2012;100(2):322–34. https://doi.org/10.1109/JPROC.2011.2144951.
[5] Zhang X, Bauer C, Mutel CL, Volkart K. Life cycle assessment of power-to-gas: approaches, system variations and their environmental implications. Appl Energy 2017;190:326–38. https://doi.org/10.1016/j.apenergy.2016.12.098.
[6] Schill W-P. Residual load, renewable surplus generation and storage requirements in Germany. Energy Pol doi:https://doi.org/10.1016/j.enpol.2014.05.032.
[7] Ozarslan A. Large-scale hydrogen energy storage in salt caverns. J Energy Storage 2012;19:14265–77. https://doi.org/10.1016/j.ijhydene.2012.07.111.
[8] Klumpp F. Comparison of pumped hydro, hydrogen storage and compressed air energy storage for integrating high shares of renewable energies – potential, cost-comparison and ranking. Int J Hydrogen Energy 2016;8:119–28. https://doi.org/10.1016/j.est.2016.09.012.
[9] Gurz M, Baltacioglu E, Hames Y, Kaya K. The meeting of hydrogen and automotive: a review. Int J Hydrogen Energy 2017;42(36):23334–223346. https://doi.org/10.1016/j.ijhydene.2017.02.124.
[10] Wilberforce T, El-Hassan Z, Khatib F, Al-Makky A, Baroutaji A, Carton J, et al. Developments of electric cars and fuel cell hydrogen electric cars. Int J Hydrogen Energy 2017;42:25695–734. https://doi.org/10.1016/j.ijhydene.2017.07.054.
[11] Simons A, Bauer C. A life-cycle perspective on automotive fuel cells. Appl Energy 2015;157:884–96. https://doi.org/10.1016/j.apenergy.2015.02.049.
[12] Weger J, Abánades A, Butler T. Methane cracking as a bridge technology to the hydrogen economy. Int J Hydrogen Energy 2017;42:720–31. https://doi.org/10.1016/j.ijhydene.2016.11.029.
[13] Miler EL. Hydrogen production & delivery program-plenary presentation-. Tech. rep. US Department of energy; 2017.
[14] Ausfelder F, Beilmann C, Bertau M, Bräuninger S, Heinze A, Hoer R, et al. Energy storage technologies as options to a secure energy supply. Chem Ing Tech 2015;87:17–73. https://doi.org/10.1002/cite.201400183.
[15] Bazanella AM, Ausfelder F. Low carbon energy and feedstock for the European chemical industry. Tech. rep., DECHEMA, 2017. URL:https://dechema.de/en/Low_carbon_chemical_industry.html [accessed June 27, 2018].
[16] Nikolaidis P, Poullikkas A. A comparative overview of hydrogen production processes. Renew Sustain Energy Rev 2017;67:597–611.
[17] Peng X. Analysis of the thermal efficiency limit of the steam methane reforming process. Ind Eng Chem Res 2012;51:16385–92. https://doi.org/10.1021/ie3002843.
[18] Spath PL, Mann MK. Life cycle assessment of hydrogen production via natural gas steam reforming. Natl Renewable Energy Lab doi:https://doi.org/10.2172/764485.
[19] Linde Engineering, Hydrogen; 2018.
[20] Santos D, Sequeira C, Figueiredo J. Hydrogen production by alkaline water electrolysis. Quim Nova 2013;36:1176–93. https://doi.org/10.1590/S0100-40422013000800017.
[21] Barbir F. Pem electrolysis for production of hydrogen from renewable energy sources. Sol Energy 2005;78:661–9. https://doi.org/10.1016/j.solener.2004.09.003.
[22] Carmo M, Fritz D, Mergel J, Stolten D. A comprehensive review on pem water electrolysis. Int J Hydrogen Energy 2013;38:4901–34. https://doi.org/10.1016/j.ijhydene.2013.01.151.
[23] Aricò A, Siracusano S, Briguglio N, Baglio V, Di Blasi A, Antonucci V. Polymer electrolyte membrane electrolysis: status of technologies and potential applications in combination with renewable power sources. J Appl Electrochem 2013;43:107–18.
[24] Schmidt O, Gambhir A, Staffell I, Hawkes A, Nelson J, Few S. Future cost and performance of water electrolysis: an expert elicitation study. Int J Hydrogen Energy 2017;42:30470–92. https://doi.org/10.1016/j.ijhydene.2017.10.045.
[25] Bernt M, Gasteiger H. Influence of ionomer content in IrO_2/TiO_2 electrodes on pem water electrolyzer performance. J Electrochem Soc 2016;163:F3179–89. https://doi.org/10.1149/2.0231611jes.
[26] Rozain C, Millet P. Electrochemical characterization of polymer electrolyte membrane water electrolysis cells. Electrochim Acta 2014;131:160–7. https://doi.org/10.1016/j.electacta.2014.01.099.
[27] Lædre S, Kongstein O, Oedegaard A, Karoliussen H, Seland F. Materials for proton exchange membrane waterelectrolyzer bipolar plates. Int J Hydrogen Energy 2017;42:2713–23. https://doi.org/10.1016/j.ijhydene.2016.11.106.
[28] Buttler A, Spliethoff H. Current status of water electrolysis for energy storage, grid balancing and sector coupling via power-to-gas and power-to-liquids: A review. Renew Sustain Energy Rev 2018;82:2440–54. https://doi.org/10.1016/j.rser.2017.09.003.
[29] Kopp M, Coleman D, Stiller C, Scheffer K, Aichinger J, Scheppat B. Energiepark mainz: technical and economic analysis of the worldwide largest power-to-gas plant with pem electrolysis. Int J Hydrogen Energy 2017;42:13311–20. https://doi.org/10.1016/j.ijhydene.2016.12.145.
[30] Lee D-Y, Elgowainy A, Dai Q. Life cycle greenhouse gas emissions of hydrogen fuel production from chlor-alkali processes in the united states. Appl Energy 2018;217:467–79. https://doi.org/10.1016/j.apenergy.2018.02.132.
[31] Utgikar V, Thiesen T. Life cycle assessment of high temperature electrolysis for hydrogen production via nuclear energy. Int J Hydrogen Energy 2006;31(7):939–44. https://doi.org/10.1016/j.ijhydene.2005.07.001.
[32] Cetinkaya E, Dincer I, Naterer G. Life cycle assessment of various hydrogen production methods. Int J Hydrogen Energy 2012;37(3):2071–80. https://doi.org/10.1016/j.ijhydene.2011.10.064.
[33] Dufour J, Serrano DP, Gálvez JL, González A, Soria E, Fierro JL. Life cycle assessment of alternatives for hydrogen production from renewable and fossil sources. Int J Hydrogen Energy 2012;37(2):1173–83. https://doi.org/10.1016/j.ijhydene.2011.09.135. [10th International Conference on Clean Energy 201].
[34] Verma A, Kumar A. Life cycle assessment of hydrogen production from underground coal gasification. Appl Energy 2015;147:556–68. https://doi.org/10.1016/j.apenergy.2015.03.009.
[35] Hajjaji N, Pons M-N, Renaudin V, Houas A. Comparative life cycle assessment of eight alternatives for hydrogen production from renewable and fossil feedstock. J Cleaner Prod 2013;44:177–89. https://doi.org/10.1016/j.jclepro.2012.11.043.
[36] Li ZWL, Zhang G. Life cycle greenhouse gas assessment of hydrogen production via chemical looping combustion thermally coupled steam reforming. J Cleaner Prod 2018;179:335–46.
[37] Ausfelder F, Dura HE. 1. Roadmap des Kopernikus-Projektes Power-to-X Flexible Nutzung erneuerbarer Ressourcen (P2X) - Optionen für ein nachhaltiges Energiesystem mit Power-to-X Technologien. Tech. rep., DECHEMA; 2018.
[38] Consoli F. SETAC, Guidelines for life-cycle assessment: a code of practice, Conference proceedings, SETAC (Society); 1993.

[39] Smolinka T, Rau S, Hebling C. Polymer electrolyte membrane (PEM) water electrolysis. Wiley-VCH,Weinheim; 2010.

[40] Suermann M, Pătrua A, Schmidt T, Büchi F. High pressure polymer electrolyte water electrolysis: test bench development and electrochemical analysis. Int J Hydrogen Energy 2017;42:12076–86. https://doi.org/10.1016/j.ijhydene.2017.01.224.

[41] Rakousky C, Reimer U, Wippermann K, Carmo M, Lueke W, Stolten D. An analysis of degradation phenomena in polymer electrolyte membrane water electrolysis. J Power Sources 2016;326:120–8. https://doi.org/10.1016/j.jpowsour.2016.06.082.

[42] Babic U, Suermann M, Buechi FN, Gubler L, Schmidt TJ. Review-identifying critical gaps for polymer electrolyte water electrolysis development. J Electrochem Soc 2017;164:F387–99. https://doi.org/10.3929/ethz-b-000190719.

[43] Luo Z, Chang Z, Zhang Y, Liu Z, Li J. Electro-osmotic drag coefficient and proton conductivity in nafion membrane for pemfc. Int J Hydrogen Energy 2010;35(7):3120–4. https://doi.org/10.1016/j.ijhydene.2009.09.013.

[44] Bensmann B, Hanke-Rauschenbach R, Arias IP, Sundmacher K. Energetic evaluation of high pressure pem electrolyzer systems for intermediate storage of renewable energies. Electrochim Acta 2013;110:570–80. https://doi.org/10.1016/j.electacta.2013.05.102.

[45] Smolinka T, Günther M, Garche J. Stand und Entwicklungspotenzial der Wasserelektrolyse zur Herstellung von Wasserstoff aus regenerativen Energien. Tech. rep. Fraunhofer ISE; 2011.

[46] Wolf M-A, Pant R, Chomkhamsrim K, Sala S, Pennington D. International reference life cycle data system (ILCD) handbook- recommendations for life cycle impact assessment in the european context. Tech. rep. European Commission-Joint Research Centre -Institute for Environment and Sustainability; 2011.

[47] Goedkoop M, Heijungs R, Huijbregts M, Schryver AD, Struijs J, van Zelm R. Recipe 2008 a life cycle impact assessment method which comprises harmonised category indicators at the midpoint and the endpoint level, Tech. rep. Ruimte en Milieu - Ministerie van Volkshuisvesting, Ruimtelijke Ordening en Milieubeheer; 2009.

[48] Feng Q, Yuan X, Liu G, Wei B, Zhang Z, Li H, et al. A review of proton exchange membrane water electrolysis on degradation mechanisms and mitigation strategies. J Power Sources 2017;366:33–55. https://doi.org/10.1016/j.jpowsour.2017.09.006.

[49] Durst J, Simon C, Haschè F, Gasteiger H. Hydrogen oxidation and evolution reaction kinetics on carbon supported Pt, Ir, Rh, and Pd electrocatalysts in acidic media. J Electrochem Soc 2015;162:F190–203. https://doi.org/10.1149/2.0981501jes.

[50] Gago S, Burggraf F, Wang L, Biermann K, Hosseini S, Gazdzicki P, et al. Zukunftspotenziale der Elektrolyse, 4.Stuttgarter EnergieSpeicherSymposium; 2015.

[51] Ito H, Maeda T, Nakano A, Hasegawa Y, Yokoi N, Hwang C, et al. Effect of flow regime of circulating water on a proton exchange membrane electrolyzer. Int J Hydrogen Energy 2010;35:9550–60. https://doi.org/10.1016/j.ijhydene.2010.06.103.

[52] Bernt M, Siebel A, Gasteiger HA. Analysis of voltage losses in pem water electrolyzers with low platinum group metal loadings. J Electrochem Soc 2018:304–14. https://doi.org/10.1149/2.0641805jes.

[53] Vierrath S, Breitwieser M, Klingele M, Britton B, Holdcroft S, Zengerle R, et al. The reasons for the high power density of fuel cells fabricated with directly deposited membranes. J Power Sources 2016;326:170–5. https://doi.org/10.1016/j.jpowsour.2016.06.132.

[54] Breitwieser M, Klose C, Klingele M, Hartmann A, Erben J, Cho H, et al. Simple fabrication of 12 μm thin nanocomposite fuel cell membranes by direct electrospinning and printing. J Power Sources 2017;337:137–44. https://doi.org/10.1016/j.jpowsour.2016.10.094.

[55] Ito H, Miyazaki N, Ishida M, Nakanoa A. Cross-permeation and consumption of hydrogen during proton exchange membrane electrolysis. Int J Hydrogen Energy 2016;41:20439–46. https://doi.org/10.1016/j.ijhydene.2016.08.119.

[56] Chandesris M, Mèdeau V, Guillet N, Chelghoum S, Thoby D, Fouda-Onana F. Membrane degradation in pem water electrolyzer: numerical modeling and experimental evidence of the influence of temperature and current density. Int J Hydrogen Energy 2015;40:1353–66. https://doi.org/10.1016/j.ijhydene.2014.11.111.

[57] Mahabunphachai S, Cora O, Koc M. Effect of manufacturing processes on formability and surface topography of proton exchange membrane fuel cell metallic bipolar plates. J Power Sources 2010;195:5269–77. https://doi.org/10.1016/j.jpowsour.2010.03.018.

[58] Trinke P, Bensmann B, Hanke-Rauschenbach R. Experimental evidence of increasing oxygen crossover with increasing current density during pem water electrolysis. Electrochem Commun 2017;82:98–102. https://doi.org/10.1016/j.elecom.2017.07.018.

[59] GmbH SV. Drying by adsorption. 2017 URL: <https://silica.berlin/en/air-and-gas-drying.html>, [accessed June 27, 2018].

[60] Dowson M, Grogan M, Birks T, Harrison D, Craig S. Streamlined life cycle assessment of transparent silica aerogel made by supercritical drying. Appl Energy 2011;97:396–404.

[61] Ayers K, Anderson E, Capuano C, Carter B, Dalton L, Hanlon G, et al. Research advances towards low cost, high efficiency pem electrolysis. ECS Trans 2010;33:3–15. https://doi.org/10.1149/1.3484496.

[62] Siemens AG. Sylizer 200 - Mit Hochdruck effizient im Megawattbereich; 2017.

[63] H-TEC Systems. Datasheet Series ME 100/350 PEM Electrolyser; 2017.

[64] Proton OnSite. Technical Specifications: M Series Hydrogen Generation Systems; 2017.

[65] Valente A, Iribarren D, Dufour J. Life cycle assessment of hydrogen energy systems: a review of methodological choices. The International Journal of Life Cycle Assessment 22; 2016.

[66] Valente A, Iribarren D, Dufour J. Harmonising the cumulative energy demand of renewable hydrogen for robust comparative life-cycle studies. J Cleaner Prod 175; 2018.

[67] Repenning J, Emele L, Blanck R, Böttcher H, Dehoust G, Förster H, et al. Klimaschutzszenario 2050, Tech. rep. Öko-Institut e.V. and Fraunhofer ISI; 2015.

[68] Kuhn P. Iteratives Modell zur Optimierung von Speicherausbau und -betrieb in einem Stromsystem mit zunehmend fluktuierender Erzeugung [Ph.D. thesis]. Technische Universität München, München; 2013.

[69] Kirchner A, Kemmler A, Wünsch M, der Maur AA, Ess F, Koziel S, et al. Klimapfade für deutschland, Tech. rep. Prognos, BCG; 2018.

[70] Bründlinger T, König JE, Frank O, Gründig D, Jugel C, Kraft P, et al. dena-Leitstudie Integrierte Energiewende: Impulse für die Gestaltung des Energiesystems bis 2050, Tech. rep. Deutsche Energie-Agentur GmbH (dena); 2018.

[71] Dorfner J, Dorfner M, Candas S, Müller S, Özsahin Y, Zipperle T, et al. urbs v0.7.3, Tech. rep., TUM; 2017. doi:https://doi.org/10.5281/zenodo.1228851.

[72] infas, DLR, Mobilität in Deutschland 2008, Tabellenband. Tech. rep., Bundesministerium für Verkehr, Bau und Stadtentwicklung; 2008.

[73] Felgenhauer M, Hamacher T. State-of-the-art of commercial electrolyzers and on-site hydrogen generation for logistic vehicles in south carolina. Int J Hydrogen Energy 2015;40(5):2084–90. https://doi.org/10.1016/j.ijhydene.2014.12.043.

[74] Matthes FC, Flachsbarth F, Loreck C, Hermann H, Falkenberg H, Cook V. ZUKUNFT STROMSYSTEM II – Regionalisierung der erneuerbaren Stromerzeugung vom Ziel her denken. Tech. rep. Umweltbundesamt; 2018.

[75] Lütkehus I, Salecker H, Adlunger K. Potential der Windenergie an Land. Tech. rep. Umweltbundesamt; 2013.

[76] Janker KA. Creation and evaluation of a database of renewable production time series and other data for energy system modelling '[Ph.D. thesis]. München: Technische Universität München; 2015.

[77] Bareiß K, Schönleber K, Hamacher T. Szenarien für den Strommix zukünftiger, flexibler Verbraucher am Beispiel von P2X-Technologien. Tech. rep. TUM - Lehrstuhl für Erneuerbare und Nachhaltige Energiesysteme; 2018.

[78] Huelsmann F, Mottschall M, Hacker F, Kasten P. Konventionelle und alternative Fahrzeugtechnologien bei Pkw und schweren Nutzfahrzeugen – Potenziale zur Minderung des Energieverbrauchs bis 2050, Tech. rep. Öko-Institute e.V.; 2014.

[79] Gniffke P. Nationale Trendtabellen für die deutsche Berichterstattung atmosphärischer Emissionen, Tech. rep., Umweltbundesamt, 2017. URL:https://www.umweltbundesamt.de/sites/default/files/medien/361/dokumente/2017_01_23_em_entwicklung_in_d_trendtabelle_thg_v1.0.xlsx, [accessed June 27, 2018].

[80] Burkhardt J, Patyk A, Tanguy P, Retzke C. Hydrogen mobility from wind energy – a life cycle assessment focusing on the fuel supply. Appl Energy 2016;181:54–64. https://doi.org/10.1016/j.apenergy.2016.07.104.

[81] Eriksson M, Ahlgren S. Lcas for petrol and diesel - a literature review. Tech. rep. Swedish University of Agricultural Science Department of Energy and Technology; 2013.

[82] Comission E. Methodology for establishing the eu list of critical raw materials – guidelines. Tech. rep. European Comission; 2017. https://doi.org/10.2873/769526.

[83] Sustainability D. TNO, British Geological Survey, Bureau de Recherches Gèologiques et Minières, Study on the review of the list of critical raw materials, Tech. rep., European Comission; 2017. doi:https://doi.org/10.2873/876644.

[84] Hagelüken C, Buchert M, Stahl H. Substantial outflows of platinum group metals identified - spent autocatalysts are systematically withdrawn from the european market. World Metall - ERZMETALL 2003;56:529–40.